American Mineralogist, Volume 73, pages 242–252, 1988

Thermochemistry of pyroxenes on the join $Mg_2Si_2O_6$-$CaMgSi_2O_6$

William D. Carlson
Department of Geological Sciences, University of Texas at Austin, Austin, Texas 78713, U.S.A.
Donald H. Lindsley
Department of Earth and Space Sciences, State University of New York, Stony Brook, New York 11794, U.S.A.

Abstract

A thermodynamic model, capable of closely replicating experimental phase equilibria in the system $Mg_2Si_2O_6$-$CaMgSi_2O_6$ over the full range of temperatures and pressures for which reversed data are now available, can be constructed employing a single asymmetric nonideal solid solution for pigeonite and diopside, a separate symmetric nonideal solid solution for orthopyroxene, and an ideal solid solution for protopyroxene. For 108 experimental brackets, ranging in temperature from 850 to 1500 °C, and ranging in pressure from 1 bar to 60 kbar, agreement between experimental and modeled compositions is within 0.02 mole fraction in 106 cases and is within 0.01 mole fraction in 85 cases. Small discrepancies exist between modeled and measured values for some calorimetric quantities and molar volume data; these could be eliminated at the cost of larger misfits in the experimental phase equilibria.

Introduction

The importance to mineralogy and petrology of pyroxenes on the join $Mg_2Si_2O_6$-$CaMgSi_2O_6$ is signified both by the great abundance of experimental phase-equilibrium data in this system and by the large number of increasingly sophisticated thermochemical models that seek to extract from those data fundamental thermodynamic properties for the pyroxene solutions. The modeling effort reported here is motivated by recent experimental data that extend our knowledge of pyroxene phase relations into regions of pressure and temperature beyond those that can be satisfactorily reproduced by the models now available.

Since the publication by Lindsley and others in 1981 of a review of data and models in this system, two important developments have occurred. First, additional high-pressure experiments not accommodated by earlier thermodynamic models have appeared (Perkins and Newton, 1980; Nickel and Brey, 1984; Brey and Huth, 1984), generating a more recent model, restricted in its applicability to high pressures (Nickel and Brey, 1984). Second, subsolidus phase relations at 1-atm pressure have been determined (Carlson, 1986, 1988) that place further constraints on mutual stabilities of the various pyroxenes in this system, also not accommodated by existing models. These low-pressure equilibria, which involve protopyroxene, lead to the necessity of incorporating this additional phase into the modeling.

Accordingly, the principal goal of this effort is to derive, from the expanded data set, thermodynamic properties that are consistent with the phase equilibria, including those involving protopyroxene, over the entire range of pressure. A successful model will allow quantitative interpolation for thermobarometric applications, provide a more reliable foundation for extrapolation to further ranges of pressure and temperature, and form a basis for extension of modeling to the quadrilateral pyroxenes and to equilibria involving additional phases.

Thermodynamic formulation

The review of Lindsley et al. (1981) includes an exposition of the theoretical aspects of thermodynamic modeling applied to Ca-Mg pyroxenes and affords a critical comparison of the approaches taken by the variety of earlier investigations of this sort. Apparent in that review is the evolution with time of increasingly more sophisticated formulations of the basic thermodynamic equalities. In their simplest form, these equalities merely require that the chemical potential for each of the two components $Mg_2Si_2O_6$ (designated here by the subscript 1) and $CaMgSi_2O_6$ (designated here by the subscript 2) must be equal in any set of pyroxenes coexisting at equilibrium. Six independent equalities relate the chemical potential of these two components in each pair of the phases protoenstatite (Pen), orthoenstatite (Oen), pigeonite (Pig), and diopside (Dio) coexisting at equilibrium. Using notation consistent with that in Lindsley et al. (1981), the conditions for equilibrium are expressed as follows:

$$0 = \mu_1^{Dio} - \mu_1^{Oen} \equiv (\mu_1^{0,Dio} - \mu_1^{0,Oen}) + RT \ln(X_1^{Dio}/X_1^{Oen}) + RT \ln(\gamma_1^{Dio}/\gamma_1^{Oen}) \quad (A)$$

$$0 = \mu_2^{Dio} - \mu_2^{Oen} \equiv (\mu_2^{0,Dio} - \mu_2^{0,Oen}) + RT \ln(X_2^{Dio}/X_2^{Oen}) + RT \ln(\gamma_2^{Dio}/\gamma_2^{Oen}) \quad (B)$$

$$0 = \mu_1^{Dio} - \mu_1^{Pig} \equiv (\mu_1^{0,Dio} - \mu_1^{0,Pig}) + RT \ln(X_1^{Dio}/X_1^{Pig}) + RT \ln(\gamma_1^{Dio}/\gamma_1^{Pig}) \quad (C)$$

0003–004X/88/0304–0242$02.00

$$0 = \mu_2^{Dio} - \mu_2^{Pig} \equiv (\mu_2^{0,Dio} - \mu_2^{0,Pig}) + RT \ln(X_2^{Dio}/X_2^{Pig}) + RT \ln(\gamma_2^{Dio}/\gamma_2^{Pig}) \quad (D)$$

$$0 = \mu_1^{Dio} - \mu_1^{Pen} \equiv (\mu_1^{0,Dio} - \mu_1^{0,Pen}) + RT \ln(X_1^{Dio}/X_1^{Pen}) + RT \ln(\gamma_1^{Dio}/\gamma_1^{Pen}) \quad (E)$$

$$0 = \mu_2^{Dio} - \mu_2^{Pen} \equiv (\mu_2^{0,Dio} - \mu_2^{0,Pen}) + RT \ln(X_2^{Dio}/X_2^{Pen}) + RT \ln(\gamma_2^{Dio}/\gamma_2^{Pen}). \quad (F)$$

Any particular formulation of the thermodynamics is characterized by the way in which it treats (a) the initial terms on the right-hand side of the above equations, which are the "standard state" terms, defining the differences in molar free energy between different pyroxene structures of the same end-member composition and (b) the final terms on the right-hand side of the above equations, which are the "excess" terms, accounting for the nonideality of each of the solid solutions. The approach taken here, described in detail below, is similar to the treatment of Lindsley et al. (1981); the reader is referred to that source for justification of the choice of this formulation. A fundamental assumption of this approach is that Pig and Dio belong to the same solid solution at high temperatures and thus obey an identical equation of state. In contrast, Oen and Pen are discrete and independent solid solutions. This model does not treat low clinoenstatite ($P2_1/c$), known to be stable below ~600 °C at 1-atm pressure (Grover, 1972) and at pressures of 75–100 kbar and above (e.g., Akaogi and Akimoto, 1977).

Thermodynamic parameters

In this formulation, the "standard-state" terms that express differences in end-member free energy are treated as linear functions of temperature and pressure and do not attempt to take into account differences in the compressibilities and expansivities of end members. Because Dio and Pig are regarded as parts of the same solid solution, the initial terms on the right hand side of Equations C and D vanish, but the corresponding terms in Equations A, B, E, and F introduce a total of twelve parameters, shown in boldface:

$$(\mu_1^{0,Dio} - \mu_1^{0,Oen}) \equiv \Delta G_A^0 \equiv \Delta \boldsymbol{U}_A^0 + P\Delta \boldsymbol{V}_A^0 - T\Delta \boldsymbol{S}_A^0$$
$$(\mu_2^{0,Dio} - \mu_2^{0,Oen}) \equiv \Delta G_B^0 \equiv \Delta \boldsymbol{U}_B^0 + P\Delta \boldsymbol{V}_B^0 - T\Delta \boldsymbol{S}_B^0$$
$$(\mu_1^{0,Dio} - \mu_1^{0,Pen}) \equiv \Delta G_E^0 \equiv \Delta \boldsymbol{U}_E^0 + P\Delta \boldsymbol{V}_E^0 - T\Delta \boldsymbol{S}_E^0$$
$$(\mu_2^{0,Dio} - \mu_2^{0,Pen}) \equiv \Delta G_F^0 \equiv \Delta \boldsymbol{U}_F^0 + P\Delta \boldsymbol{V}_F^0 - T\Delta \boldsymbol{S}_F^0.$$

The nonideal mixing properties of each solution are described by the final terms on the right-hand side of Equations A–F using activity coefficients, but may equivalently be expressed as explicit functions of composition by employing Margules interaction parameters (cf. Thompson, 1967). In this formulation, an asymmetric solution incorporating both temperature and pressure dependence is adopted for clinopyroxene, so that the excess molar free energy of mixing is given by

$$G_{xs}^{Cpx} \equiv (W_{G_1}^{Cpx})(X_1^{Cpx})(X_2^{Cpx})^2 + (W_{G_2}^{Cpx})(X_2^{Cpx})(X_1^{Cpx})^2$$
$$\equiv (\boldsymbol{W}_{U_1}^{Cpx} + P\boldsymbol{W}_{V_1}^{Cpx} - TW_{S_1}^{Cpx})(X_1^{Cpx})(X_2^{Cpx})^2$$
$$+ (\boldsymbol{W}_{U_2}^{Cpx} + P\boldsymbol{W}_{V_2}^{Cpx} - TW_{S_2}^{Cpx})(X_2^{Cpx})(X_1^{Cpx})^2.$$

Treating the temperature dependence of the Margules parameters as a symmetric property permits the simplification

$$\boldsymbol{W}_S^{Cpx} \equiv W_{S_1}^{Cpx} = W_{S_2}^{Cpx}$$

and thus reduces the number of parameters used to describe the clinopyroxene solution properties to five, again in boldface above.

Orthopyroxene is regarded as a symmetric solution. The nonideal mixing properties are treated as explicit functions of pressure, thereby introducing two additional parameters:

$$G_{xs}^{Oen} \equiv (W_G^{Oen})(X_1^{Oen})(X_2^{Oen}) \equiv (\boldsymbol{W}_A^{Oen} + P\boldsymbol{W}_V^{Oen})(X_1^{Oen})(X_2^{Oen}).$$

Protopyroxene is likewise regarded as a symmetric solution, but without explicit temperature or pressure dependence. Thus a single additional parameter suffices to treat its solution properties:

$$G_{xs}^{Pen} \equiv (\boldsymbol{W}_G^{Pen})(X_1^{Pen})(X_2^{Pen}).$$

Experimental constraints.

Each experimental datum that specifies the compositions of two coexisting pyroxenes at a particular temperature and pressure constitutes a requirement that the parameters of the model take on particular values; the values must be those that simultaneously satisfy (after appropriate substitution of P, T, and two X's) a pair of thermodynamic equations (either A and B, C and D, or E and F, depending on the identity of the phases). The number of reversed experimental data in this system is large, and data are now available over an exceptionally wide range of both temperature and pressure, as illustrated by the compilation in Table 1. Synthesis results are not included.

The experiments of Mori and Green (1975), Lindsley and Dixon (1976), Perkins and Newton (1980), Schweitzer (1982), Brey and Huth (1984), and Nickel and Brey (1984) all yielded products with nonuniform compositions. In nearly all cases, reversal runs in which equilibrium compositions were approached simultaneously from two directions generated regions of overlap in product compositions. This presumably results from excessive overstepping of the reaction, which can produce nucleation of crystals with compositions lying on the side of the equilibrium composition that is opposite to the metastable reactants [the phenomenon of "path-looping" described by Perkins and Newton (1980, p. 293)]. For these experiments, it has been conventional to regard the limits of the zone of overlapping compositions as the experimental bracket, and the same convention is followed here. But this possibility of path-looping makes interpretation of half-reversal runs, in which the equilibrium composition is approached from one side only, extremely difficult. In the absence of path-looping, such a run would be expected to drive a reactant composition in one direction only, so that the resulting composition could be treated as a maximum or minimum limiting the equilibrium

TABLE 1. Mole fraction $CaMgSi_2O_6$ in coexisting pyroxenes

P (kbar)	*T* (°C)	Phase	Min.	Max.	Calc.	Source
0.001	925	Oen		0.023	0.020	C
		Dio	0.899		0.908	
	975	Oen	0.024	0.026	0.026	C
		Dio	0.879	0.885	0.891	
	1025	Pen	0.022	0.026	0.022	C
		Dio	0.843	0.862	0.874*	
	1075	Pen	0.023	0.026	0.025	C
		Dio	0.838	0.844	0.855*	
	1125	Pen	0.025	0.027	0.028	C
		Dio	0.828	0.834	0.834	
	1175	Pen	0.027	0.033	0.031	C
		Dio	0.796	0.806	0.809	
	1225	Pen	0.032	0.033	0.033	C
		Dio	0.767	0.785	0.781	
	1275	Pen	0.035	0.039	0.036	C
		Dio	0.745	0.751	0.748	
	1295†	Pen	0.033	0.036	0.037	C
		Pig	0.160	0.173	0.159	
		Dio	0.733	0.741	0.735	
	1325	Pen	0.030	0.034	0.037	C
		Pig	0.137	0.144	0.151	
	1350	Pen	0.029	0.035	0.037	C
		Pig	0.119	0.130	0.146*	
	1325	Pig	0.182	0.189	0.175	C
		Dio	0.702	0.730	0.713	
	1350	Pig	0.197	0.201	0.189	C
		Dio	0.681	0.695	0.695	
	1375	Pig	0.210		0.203	C
		Dio		0.680	0.677	
2.0	1200	Oen	0.077	0.090	0.074	WL
		Dio	0.789	0.805	0.790	
5.0	1200	Oen	0.070	0.090	0.068	LD
		Dio	0.770	0.790	0.792	
10.0	900	Oen	0.028	0.042	0.016*	MG
		Dio	0.878	0.932	0.919	
15.0	850	Oen	0.010	0.010	0.012	LD
		Dio	0.930	0.940	0.934	
	1000	Oen	0.030	0.030	0.026	LD
		Dio	0.900	0.910	0.890	
	1100	Oen	0.040	0.050	0.039	LD
		Dio	0.850	0.880	0.851	
	1200	Oen	0.060	0.060	0.056	LD
		Dio	0.840	0.850	0.802**	
	1300	Oen	0.080	0.090	0.077	LD
		Dio	0.740	0.770	0.736	
	1400	Oen	0.110	0.110	0.099*	LD
		Dio	0.590	0.650	0.634	
	1465‡	Oen	0.090	0.130	0.108	S
		Pig	0.336	0.396	0.317*	
		Dio	0.500	0.640	0.559	
20.0	900	Oen	0.024	0.025	0.015	LD
		Dio	0.930	0.940	0.923	
	900	Oen	0.012	0.030	0.015	PN
		Dio	0.930	0.946	0.923	
25.0	900	Oen	0.016	0.020	0.015	PN
		Dio	0.938	0.946	0.925*	
	1000	Oen	0.024	0.030	0.024	PN
		Dio	0.910	0.916	0.895*	
	1100	Oen	0.022	0.028	0.035	PN
		Dio	0.870	0.884	0.858*	
30.0	900	Oen	0.016	0.016	0.014	MG
		Dio	0.928	0.934	0.927	
	900	Oen	0.010	0.012	0.014	PN
		Dio	0.940	0.940	0.927*	
	1000	Oen	0.018	0.032	0.023	PN
		Dio	0.904	0.916	0.898	
	1100	Oen	0.026	0.028	0.034	PN
		Dio	0.866	0.892	0.861	
	1200	Oen	0.048	0.062	0.046	MG
		Dio	0.842	0.884	0.816**	
	1500	Oen	0.100	0.104	0.091	MG
		Dio	0.550	0.578	0.524**	
	1500	Oen	0.108	0.110	0.091*	NB
		Dio	0.456	0.654	0.524	
40.0	1200	Oen	0.034	0.038	0.042	BH
		Dio	0.842	0.872	0.824*	
	1300	Oen	0.052	0.052	0.054	BH
		Dio	0.780	0.794	0.769*	
	1500	Oen	0.092	0.098	0.079*	NB
		Dio	0.524	0.574	0.587*	
50.0	900	Oen	0.006	0.008	0.013	NB
		Dio	0.914	0.948	0.933	
	1100	Oen	0.023	0.032	0.029	BH
		Dio	0.872	0.894	0.874	
	1200	Oen	0.032	0.032	0.038	BH
		Dio	0.842	0.880	0.832	
	1300	Oen	0.046	0.048	0.049	BH
		Dio	0.784	0.816	0.780	
	1400	Oen	0.063	0.063	0.060	BH
		Dio	0.724	0.752	0.713*	
	1500	Oen	0.086	0.086	0.071*	BH
		Dio	0.586	0.608	0.624*	
60.0	1300	Oen	0.036	0.038	0.045	BH
		Dio	0.788	0.828	0.791	

Note: Abbreviations: BH = Brey and Huth (1984); C = Carlson (1986, 1988); LD = Lindsley and Dixon (1976); MG = Mori and Green (1975); NB = Nickel and Brey (1984); PN = Perkins and Newton (1980); S = Schweitzer (1982); WL = Warner and Luth (1974).

* Misfit > 0.01 mole fraction.

** Misfit > 0.02 mole fraction.

† Model compositions for the calculated three-phase equilibrium at 1292 °C.

‡ Model compositions for the calculated three-phase equilibrium at 1436 °C.

composition. If path-looping occurs, however, this is no longer the case. In fact, any pair of runs that constitutes a two-sided reversal with overlapping compositions would yield two *mutually inconsistent* limits. For this reason, data from the above sources on half-reversal runs are not included in the compilation of Table 1; also excluded for the same reason are the results of Nehru and Wyllie (1974) and Mori and Green (1976). (More than half of these one-sided brackets turn out to be in agreement with the model presented below.) Only one other experimental datum is excluded from Table 1. The experiment by Brey and Huth (1984) at 1500 °C, 40 kbar was repeated and found to be

in error by Nickel and Brey (1984); the earlier result is therefore replaced by the latter in the above compilation.

Further constraints are provided by two determinations of the temperature for the conversion of end-member magnesian Oen to Pen. At 1-bar pressure, the data of Atlas (1952), Smyth (1974), and others locate the transition at 975 ± 10 °C; at 8-kbar pressure, the data of Chen and Presnall (1975) reverse the transition between 1313 °C and 1417 °C.

Procedure and results

If each experiment in Table 1 specified a unique pair of compositions for the coexisting pyroxenes, then the 53 experiments in the table would overdetermine a system of only 20 variables. Instead, the data set is unavoidably ambiguous because of the uncertainty inherent in any experimentally determined compositional bracket. Attempts to extract thermodynamic quantities from such data by the commonly used technique of least-squares regression require that this uncertainty be ignored (or accommodated by assignment of zero error to any calculated composition falling within a given interval of the bracket center, as suggested by Davidson, pers. comm.). Thus with the least-squares technique, it is necessary to designate a particular single value lying within the bracket as the "correct" value to which the model will be fit. The choice of the midpoints of the brackets (e.g., Holland et al., 1979; Nickel and Brey, 1984) provides a unique selection, but that choice may not yield optimum values for the parameters, necessitating instead a trial-and-error process involving successive refinements of choices for the "correct" experimental datum (cf. Lindsley et al., 1981, p. 165–166). To circumvent this problem, we have used the technique of linear programming, which accounts explicitly for the uncertainties inherent in each pair of experimental brackets.

Linear programming technique

The use of linear programming methods to extract thermodynamic data from experimental results is not new (cf. Gordon, 1977; Day and Halbach, 1979; Day and Kumin, 1980; Berman and Brown, 1984), but the method has not been widely applied to date. The linear programming algorithms permit any linear function of the thermodynamic parameters (the "objective function") to be maximized, subject to inequality constraints cast as linear combinations of those parameters. The constraints arise directly from the experimental data by the conversion of the thermodynamic equations of equilibrium (Eqs. A–F) into thermodynamic *inequalities*. Each equation of the type A through F can be translated into a pair of inequalities, representing the widest and narrowest pairs of compositions permitted by the bracket. For example, an experiment bracketing the compositions of coexisting Oen + Dio converts Equation A into these inequalities:

$$0 < (\mu_1^{0,\mathrm{Dio}} - \mu_1^{0,\mathrm{Oen}}) + RT \ln(X_{1,\max}^{\mathrm{Dio}}/X_{1,\min}^{\mathrm{Oen}}) + RT \ln(\gamma_1^{\mathrm{Dio}}/\gamma_1^{\mathrm{Oen}})$$

$$0 > (\mu_1^{0,\mathrm{Dio}} - \mu_1^{0,\mathrm{Oen}}) + RT \ln(X_{1,\min}^{\mathrm{Dio}}/X_{1,\max}^{\mathrm{Oen}}) + RT \ln(\gamma_1^{\mathrm{Dio}}/\gamma_1^{\mathrm{Oen}})$$

in which the subscripts max and min designate the most Mg-rich and most Ca-rich compositions permitted by the brackets. (The same combination of max and min values used in the second term also enters the third term when the $RT \ln \gamma_1$ entries are expanded into the Margules G_{xs} entries.)

The linear programming technique presumes that the thermodynamic parameters can vary over a range of values while still satisfying the constraining inequalities. The algorithm then determines the particular values in that range that maximize the arbitrarily chosen objective function. The currently available data, if applied uncritically, are sufficiently contradictory (at the level of complexity of all present models) to render the linear programming problem insoluble; that is, no combination of values for the parameters can rigorously satisfy those constraints. The procedure that is required in this case is to selectively relax (or eliminate) some of the experimental limits until the contradictions in the constraints are removed. The end result is a tightly constrained situation in which most parameters will vary only slightly in response to different choices of the objective function. The objective function can then be chosen to deflect the solution toward results that are not explicit in the structure of the constraints, as for example, to improve correspondence with calorimetric or crystallographic measurements.

This technique is not without drawbacks. One of these is the requirement (in most implementations of the algorithm) that parameters be assigned a priori to either positive or negative values. This is inconvenient, but is easily rectified by changing the sign of any parameter that is driven to a zero value by a particular choice of the objective function and the repeating the solution. Another difficulty arises from the fact that the structure of the thermodynamic inequalities forces constraints to be written in terms of *ratios* of phase compositions. This permits solutions to exist for which the compositions calculated for coexisting pyroxenes will both fall at higher values (or both at lower values) than desired; when this occurs, the ratio of compositions satisfies the constraint, even though either one or both of the calculated compositions may violate its bracket. This difficulty may be averted by selectively tightening the limits on the input brackets until agreement is obtained. A third complication arises in treating three-pyroxene equilibria, which must be regarded as three independent *pairs* of brackets. It is possible for the constraints imposed by different pairs to be satisfied by differing pyroxene compositions, which nevertheless fit within the brackets. Thus, for example, a model can satisfy each pair of experimental constraints by calculating, at the equilibrium temperature, one Pig composition (near the magnesian end of the bracketed range) for Pig in equilibrium with Oen, and a distinct Pig composition (near the calcic end of the bracket) for Pig in

TABLE 2. Model values for thermodynamic parameters

Parameter	Optimum	Max.	Min.
ΔU^0_A	4.261	4.810	3.973
ΔV^0_A	0.05900	0.06011	0.05710
ΔS^0_A	2.721	3.028	2.517
ΔU^0_B	−35.92	−32.55	−35.92
ΔV^0_B	−1.753	−1.618	−1.753
ΔS^0_B	−20.97	−19.46	−20.97
ΔU^0_E	0.9814	1.7082	0.8302
ΔV^0_E	−0.07954	−0.05246	−0.07954
ΔS^0_E	0.09328	0.54244	0.0
ΔU^0_F	−36.71	0.0	−40.52
ΔV^0_F	0.0	0.0	−40520.0
ΔS^0_F	2.444	10.155	0.053
W^{Cpx}_{U1}	26.23	26.29	25.50
W^{Cpx}_{U2}	32.44	32.44	31.84
W^{Cpx}_{V1}	−0.02229	−0.01571	−0.02382
W^{Cpx}_{V2}	−0.08646	−0.08201	−0.09301
W^{Cpx}_{S}	0.0	0.0	−0.3961
W^{Pen}_{A}	28.60	30.03	28.60
W^{Pen}_{V}	−1.749	−1.607	−1.749
W^{Pen}_{G}	0.0	9.239	0.0

Note: Energy in kJ·mol^{-1}; volume in kJ·kbar^{-1}·mol^{-1}; entropy in J·K^{-1}·mol^{-1}.

equilibrium with Dio. In this situation, the calculated three-phase equilibrium lies at a temperature different from that of the experiment. The discrepancy in temperature decreases as the width of the constraining brackets is reduced, so that tightening of the input brackets will force the model closer to the empirically determined temperature for the three-phase equilibrium.

Fitting of parameters

Despite the flexibility of the linear programming technique, the mutual contradictions present within the data set are large enough to prevent a strict adherence to all of the available constraining data. Thus, as noted above, there is *no* set of values for the parameters that will bring this thermodynamic formulation into rigorous agreement with all of the constraints simultaneously. Consequently, this model, like all others, represents an attempt to reach a compromise that, while violating some experimental brackets, nevertheless succeeds in reproducing quantitatively the essential features of the phase equilibria.

To reach this compromise, the original constraints were selectively modified. The first step was to remove from the set of constraints a few experimental brackets that consistently appeared discrepant (by >0.02 mole fraction) with the rest of the data, regardless of how the model was varied. Next, some brackets that were in general agreement with remainder of data, but that placed unduly rigid constraints on the outcome, were expanded slightly. In this way, allowance of small misfits in these brackets avoided much larger misfits elsewhere. Finally, small adjustments were made, tightening some brackets in order to achieve a balanced partitioning of discrepancies and to minimize the total extent of misfit. (No attempt was made to evaluate the relative quality of published results, and thereby to weight the fit toward a particular portion of the data set at the expense of greater misfits elsewhere.) In this adjustment process, it became clear that slight changes in the parameters can be made to produce excellent fits in any arbitrarily chosen pressure range, but only at the expense of increasing misfits at other pressures or introducing equilibria contrary to known stabilities (e.g., predicting $CaMgSi_2O_6$ stable in the orthorhombic structure at $T < 1385$ °C). Implicit in this procedure is the notion that the primary criterion for judging the model is its ability to reproduce the experimentally determined phase equilibria.

Results

The second column of Table 2 lists preferred values for the thermochemical parameters. The objective function used to obtain this solution maximized the free-energy difference between the orthorhombic and monoclinic forms of $CaMgSi_2O_6$ at high temperature and low pressure. This was done to ensure that the temperature at which "orthodiopside" is calculated to become stable lies in the supersolidus range. The two rightmost columns in Table 2 indicate the range of values over which solutions consistent with the constraints can be found. These ranges were determined by repeatedly solving the linear programming problem, using the same set of constraints employed to obtain the preferred model, but altering the objective function in successive solutions to maximize, then minimize, each of the parameters individually.

The magnitude of the range of acceptable values for each parameter is an indication of how tightly the experimental data constrain that parameter. Some parameters (e.g., W^{Cpx}_{U1}, W^{Cpx}_{U2}) cannot vary greatly from the preferred value without violating one of the experimental brackets; others (e.g., W^{Pen}_{G}, ΔV^0_F) lack strong constraints in the data set and are therefore capable of considerable variability. The ranges listed are not, however, rigorous measures of the uncertainty in the parameters. Because some of the parameters are closely correlated with one another, the choice of an extreme value for one may require, in order to fit the experimental data, a particular (often extreme) value of another variable. Thus a set of values selected arbitrarily, all of which fall within the given ranges, may well *not* generate an acceptable fit to the experimental data. Nevertheless, for the particular set of constraints employed, any value for a parameter that lies outside the stated range will not generate an acceptable solution, regardless of the values chosen for the other parameters.

As a consequence of the choice of objective function, three of the parameters take on values of zero in the preferred model. This is appropriate for ΔV^0_F, which is almost completely unconstrained by the experimental data. It is likewise appropriate for W^{Cpx}_{S}, which takes on small values of either sign in nearly all successful variations on the preferred model. However, a value of zero for W^{Pen}_{G}, which implies that the protopyroxene solution is ideal, is contrary to expectation. Although the protopyroxene so-

lution is probably nonideal, the available data do not constrain the solution properties sufficiently to place useful limits on the degree of nonideality of the solution. Considering that the available data are in fact consistent with ideal-mixing properties for protopyroxene, it was decided to adopt the simpler ideal model in preference to one that would assign a poorly constrained nonideal value to the mixing parameter. An arbitrary assignment of any value up to about 10 kJ/mol to W_G^{Pen} does not materially affect the ability of the model to replicate the experimental data.

Thermometric expressions

The temperature of equilibration T (in degrees Celsius) represented by coexisting orthopyroxene and clinopyroxene in this system at pressure P (in kilobars) is obtained by rearrangement of Equations A and B into the form

$$T_A = -273.15 + \frac{4.261 + 0.05900P + W_{G1}^{Cpx}(X_2^{Cpx})^2(1 - 2X_1^{Cpx}) + 2W_{G2}^{Cpx}(X_1^{Cpx})(X_2^{Cpx})^2 - W_G^{Oen}(X_2^{Oen})^2}{0.002\,721 - R\ln(X_1^{Cpx}/X_1^{Oen})}$$

$$T_B = -273.15 + \frac{-35.92 - 1.753P + W_{G2}^{Cpx}(X_1^{Cpx})^2(1 - 2X_2^{Cpx}) + 2W_{G1}^{Cpx}(X_2^{Cpx})(X_1^{Cpx})^2 - W_G^{Oen}(X_1^{Oen})^2}{-0.02097 - R\ln(X_2^{Cpx}/X_2^{Oen})}$$

where $R = 0.008\,314\,3$; $W_{G1}^{Cpx} = 26.23 - 0.02229P$; $W_{G2}^{Cpx} = 32.44 - 0.08646P$; and $W_G^{Oen} = 28.60 - 1.749P$.

Discussion

Fit to experimental data

The preferred values for the model parameters were used to calculate the phase diagrams shown in Figures 1a–1g, and numerical comparisons of the published experimental brackets with compositions calculated from the model are made in Table 1. This table includes all of the available constraints in their original form, ignoring any modifications made during the fitting procedure. The results demonstrate that the model readily achieved at least two of its principal goals.

First, it proved possible to incorporate protopyroxene equilibria into the system and to extract values for the end-member free-energy differences that are consistent with the available experimental constraints. As expected, protopyroxene-bearing equilibria are calculated by the model to become unstable at pressures slightly in excess of 10 kbar, and protopyroxene compositions are restricted to the extremely Mg-rich portions of the system.

Second, it proved possible to achieve a satisfactory fit to all of the existing experimental data in the system over the entire range of pressure. Of the 108 brackets listed, 85 are fit to within 0.01 mole fraction; 106 are fit to within 0.02 mole fraction. The most difficult constraint to fit in this data set is the 15-kbar equilibrium among Oen, Pig, and Dio, placed at 1465 ± 10 °C. Because, under these conditions, the compositions of the clinopyroxenes change extremely rapidly with temperature (cf. Fig. 1b), differences that are large in terms of mole fraction correspond to decidedly smaller differences in temperature. A misfit of less than 0.02 mole fraction can be achieved for this constraint if the same compositional ranges are regarded to lie at the calculated temperature for this three-phase equilibrium, which is 1436 °C, or 19 °C below the published limits of error. [Both Kushiro and Yoder (1970) and Mori and Green (1975), relying primarily on synthesis results, suggested that this three-phase equilibrium at 15 kbar lies at about 1425 °C.]

Comparison with other constraints

Calorimetry. The calorimetric measurements of Newton et al. (1979) provide enthalpy of solution measurements for the clinopyroxenes extending in composition from end-member diopside to 0.22 mole fraction $CaMgSi_2O_6$. Employing a quadratic extrapolation of these data to the monoclinic magnesian end-member, those authors indicate a value of 8.4 ± 4.2 kJ/mol for ΔU_A^0, whereas the present model yields a preferred value of 4.26 kJ/mol and a maximum value of 4.81 kJ/mol. Like the other discrepancies, this marginal agreement may be a genuine reflection of the compromises among conflicting data required by an insufficiently complex model. Models designed to alleviate this discrepancy [e.g., the preliminary model of Carlson and Lindsley (1986), with ΔU_A^0 at ~8 kJ/mol] produce significantly poorer fits to the 1-bar pigeonite-bearing equilibria and to the brackets above 1400 °C at 40 and 50 kbar. Alternatively, the explanation may again be the one advanced originally by Lindsley et al. (1981, p. 171–172) to address the identical problem in their model: because of the possibility that the calorimetric measurements were carried out at a temperature below that at which pigeonite assumes $C2/c$ symmetry, the difference between measured and modeled values may represent the enthalpy of the transition from $P2_1/c$ to $C2/c$ for pigeonite.

Molar volume. Additional constraints are provided by measurements of molar volumes for orthopyroxene and protopyroxene at the $Mg_2Si_2O_6$ end member and by extrapolation to that end member of molar-volume measurements made on $C2/c$ clinopyroxene.

The difference in molar volume between orthoenstatite and protoenstatite, based upon the data of Hawthorne and Ito (1977) and Smith (1969), respectively, is 0.214 kJ/kbar at 25 °C and 1 bar. The modeling yields a preferred value (given by the difference $\Delta V_A^0 - \Delta V_E^0$) of 0.139 kJ/kbar; an alternative solution maximizing this value gives 0.140 kJ/kbar. This discrepancy is very likely a consequence of the failure of the present thermodynamic for-

mulation to include compressibilities and expansivities for the end members. Because of its unusually elongated c dimension, protopyroxene may have markedly different volume responses to temperature and pressure than do the other two structures. Failure to acknowledge this in the thermodynamic formulation (i.e., the need for single values for ΔV_A^0 and ΔV_E^0 that apply over the entire range of pressure and temperature) may be the reason that the Oen = Pen transition curve is forced in nearly all successful variations of the model to its minimum allowable slope.

Published measurements of the molar volume for Ca-Mg clinopyroxene extend from the calcic end member down to 0.22 mole fraction $CaMgSi_2O_6$ (Newton et al., 1979), but the extrapolated value at $Mg_2Si_2O_6$ is uncertain. Nickel and Brey (1984, p. 36–37) have argued that a straightforward quadratic extrapolation to the magnesian end member will underestimate the molar volume there, and they have proposed that a likely range for the difference in molar volume between the clinopyroxene structure and the orthopyroxene structure at $Mg_2Si_2O_6$ is -0.01 to $+0.07$ kJ/kbar. The modeled value for ΔV_A^0 of $+0.059$ kJ/kbar falls comfortably within this range, very close to the value fitted by Nickel and Brey (1984) and somewhat above the value resulting from the earlier fit of Lindsley et al. (1981). The preferred value is substantially larger than the slightly negative value arising from the quadratic regression on the volume data performed by Newton et al. (1979).

Comparison with previous thermodynamic models

Table 3 affords a comparison among recent thermochemical models for orthopyroxene and clinopyroxene in the system $Mg_2Si_2O_6$-$CaMgSi_2O_6$. The various models are derived from overlapping but distinct sets of experimental data. The overlap among data sets accounts for the generally good agreement seen in Table 3, whereas the distinctions among data sets (principally in the range of pressure for which phase-equilibrium data were included) account for the differences that do appear among the models. It is noteworthy that whereas solution parameters for orthopyroxene are poorly constrained in the two earlier models, which included only data on coexisting orthopyroxene and clinopyroxene, they are reasonably well determined in the two later models, which incorporate protopyroxene equilibria as well.

Calculated univariant phase equilibria

The projections onto the P-T plane of calculated univariant equilibria among the four pyroxene phases considered in this model are presented in Figure 2. Equilibria in the Ca-free system are shown by light lines and are constrained by the results of Atlas (1952) and Chen and Presnall (1975), indicated by open rectangles. Equilibria among Ca-bearing phases are shown by bold lines and are constrained by the data of Carlson (1985, 1986, 1988) and of Schweitzer (1982), both indicated by solid rectangles. The dashed line is the projection of the consolute curve along which Pig = Dio. The univariant equilibrium Oen + Dio = Pig terminates, at its intersection with the dashed consolute curve, in a critical endpoint near 1450 °C and 18 kbar.

The position and arrangement of the four univariant curves that radiate from the invariant point near 1240 °C and 1.2 kbar are of particular interest, because of the puzzling presence of orthoenstatite, or a distinct orthoenstatite-like phase, in 1-bar experiments in the temperature range 1370 °C to 1445 °C (cf. Longhi and Boudreau, 1980; Carlson, 1988). In order for orthoenstatite to regain stability at and above 1370 °C at atmospheric pressure, the equilibrium Oen = Pen + Pig must intersect the 1-atm isobar at 1370 °C, after departing the invariant point with a steeper dP/dT slope than that of the equilibrium Oen = Pen + Dio. An unexpected and intriguing result of this model is that substantial curvature is present along the latter equilibrium, enough in fact to generate a subtle pressure maximum along it and to cause it to arrive at the invariant point with shallow negative slope. Once this fact was recognized, a thorough attempt was made to incorporate, in the model's constraints, stability fields near 1400 °C at atmospheric pressure for coexisting Pen + Oen and Oen + Pig, based on the synthesis data of Carlson (1988). Although it was possible to generate models with appropriate compositions for these coexisting pyroxenes that gave moderately good agreement with the remainder of the data set, all such models predicted that the Oen-bearing assemblages would be metastable with respect to the pair Pen + Pig. Therefore, the reaction of Pen + Pig to produce Oen at 1370 °C at atmospheric pressure is, *within the limits of the present formulation of the ther-*

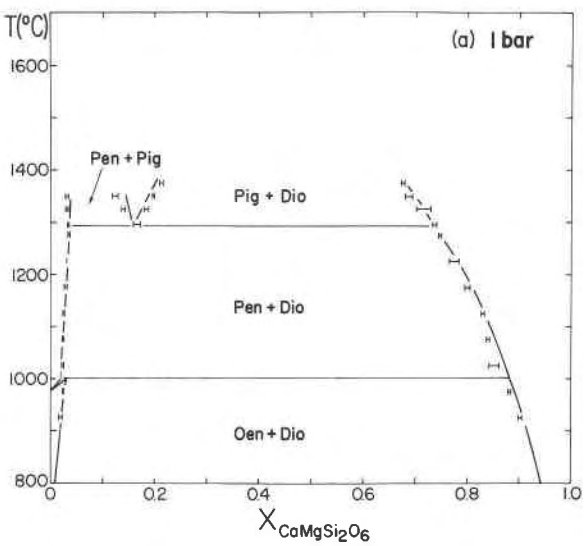

→

Fig. 1. Calculated phase equilibria compared to experimental constraints for pressures of (**a**) 1 bar and (**b**) 15, (**c**) 20, (**d**) 25, (**e**) 30, (**f**) 40, and (**g**) 50 kbar. Sources of experimental data given in Table 1.

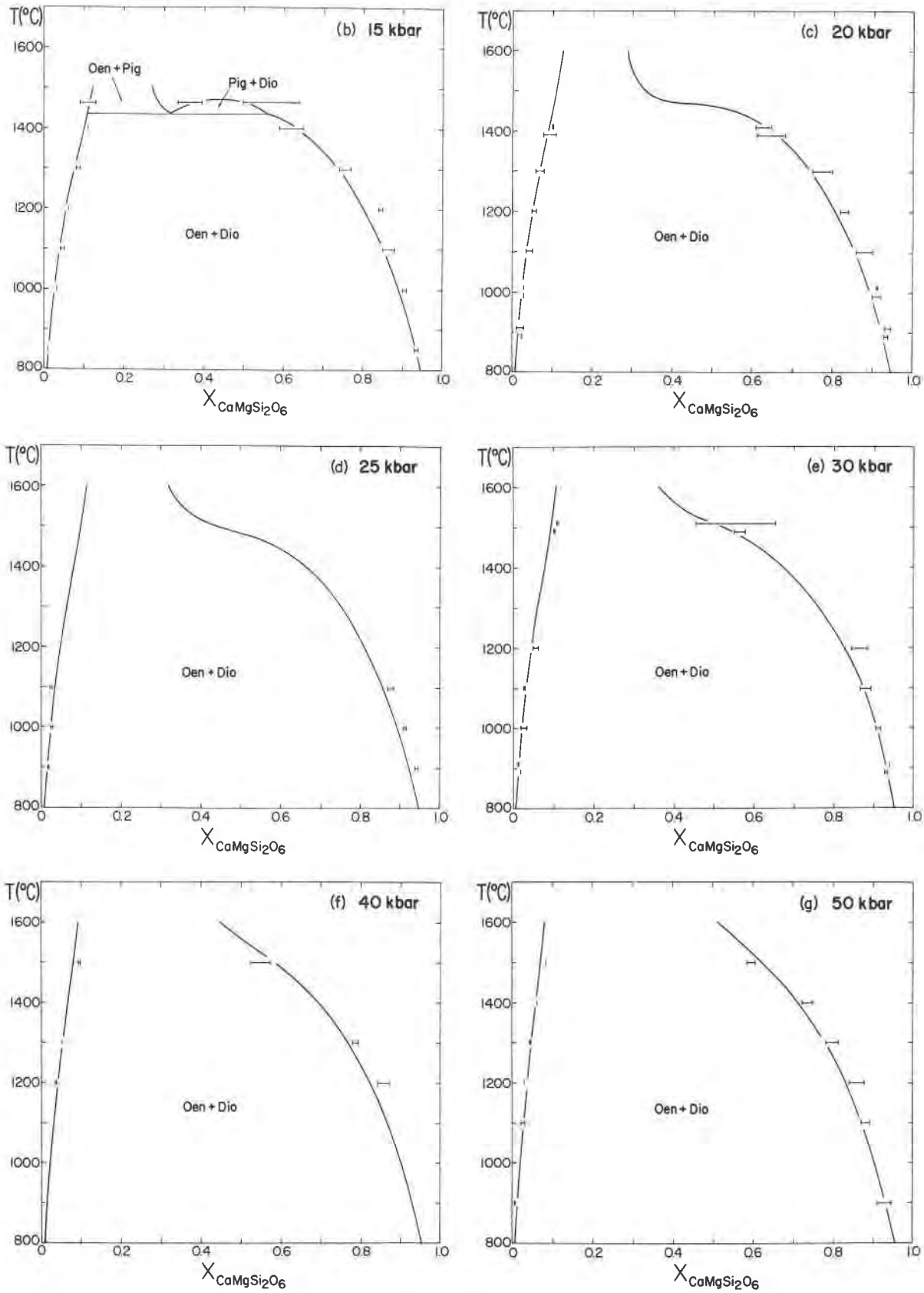

Fig. 1—*Continued.*

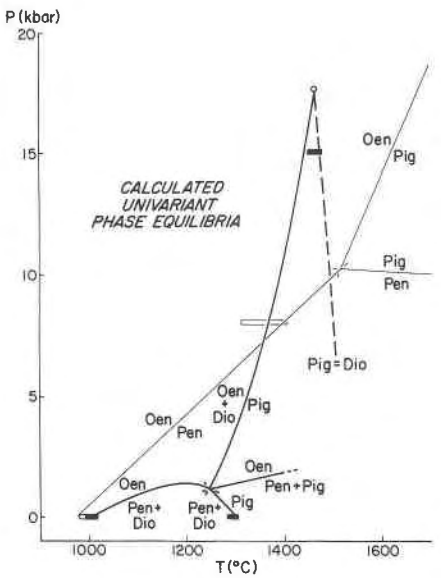

Fig. 2. Calculated univariant phase equilibria. Light lines portray equilibria in the end-member Ca-free system; bold lines portray equilibria among Ca-bearing solid solutions. Complex supersolidus phase relations predicted by the model at $P < 5$ kbar and $T > 1400$ °C are not shown (see text for discussion).

TABLE 3. Thermodynamic parameters for clinopyroxene-orthopyroxene equilibria

Parameter	LGD	NB	CL	This study
ΔU^0_A	3.561	7†	7.96	4.261
ΔV^0_A	0.0355	0.06188	0.107	0.05900
ΔS^0_A	1.91	3.97	5.44	2.721
ΔU^0_B	−21.178	−12.909	−56.5	−35.92
ΔV^0_B	−0.0908	−0.1633	−2.06	−1.753
ΔS^0_B	−8.16	−8.50	−28.6	−20.97
W^{CPX}_{U1}	25.484	21.905*	24.4	26.23
W^{CPX}_{U2}	31.216	21.905*	32.4	32.44
W^{CPX}_{V1}	0.0812	−0.05229*	−0.0366	−0.02229
W^{CPX}_{V2}	−0.0061	−0.05229*	−0.160	−0.08646
W^{CPX}_{S}		−4.43	−0.834	0.0
W^{OEN}_{A}	25†	34†	15.7	28.60
W^{OEN}_{V}			−1.97	−1.749

Note: Energy in kJ·mol^{-1}; volume in kJ·kbar^{-1}·mol^{-1}; entropy in J·K^{-1}·mol^{-1}. Abbreviations: LGD = Lindsley et al., 1981; NB = Nickel and Brey, 1984; CL = Carlson and Lindsley, 1986.

* Symmetric parameter.

† Fixed value, not fitted.

modynamics, inconsistent with the remainder of the experimental data.

The calculation of a positive dP/dT slope for the equilibrium Oen = Pen + Pig should not, however, be construed as apodictic evidence against the high-temperature stability of orthoenstatite at atmospheric pressure. In fact, as described in more detail in the following section, this model does generate a high-temperature, low-pressure stability field for Oen, but at temperatures slightly too high and at compositions substantially too calcic to be in agreement with the phase-equilibrium data now available. Equilibria among these low-Ca pyroxenes are not tightly constrained by the experimental data set; moderate adjustments in the values of the parameters perturb the position of the univariant curve substantially. Thus it may still be possible, in the context of a more elaborate or sophisticated formulation of the thermodynamics, to account for a split stability field for orthoenstatite at atmospheric pressure by the intersection of the equilibrium Oen = Pen + Pig with the 1-atm isobar.

Limitations of the model

Systematic misfits. Even after exclusion of inconsistent constraints, it did not prove possible, using this particular thermodynamic formulation, to simultaneously meet all of the constraints imposed by the published experimental data. The infeasibility of rigorously replicating all experimental results suggests either that the data are not absolutely internally consistent, or that the chosen thermodynamic approach omits critical parameters, or both. Although inconsistency in a data set arising from so many different sources is not unlikely, the fact that the misfits evident in this model are somewhat systematic may indicate that the model is indeed an insufficiently complex compromise among a number of competing factors.

Although the calculations are in excellent agreement with experiment at temperatures from 800 °C to approximately 1100 °C at all pressures, systematic discrepancies occur at higher temperatures. The calculated miscibility gap between orthoenstatite and diopside is consistently slightly too narrow near 1200–1300 °C and consistently slightly too wide above about 1400 °C; the effect is more pronounced at higher pressures. In an attempt to eliminate this minor problem, the thermodynamic formulation was expanded to include a W^{Oen}_S term, generating a temperature dependence for the nonideality of the orthopyroxene solution. This attempt was unsuccessful. The systematic discrepancies can be reduced by suitable small changes in the values for the model parameters, but only at the expense of markedly worsening the misfits in pigeonite compositions at 1 bar, or the discrepancy in temperature of the three-phase equilibrium at 15 kbar, or both. The preferred model compromises among these possibilities.

Supersolidus equilibria at low pressures. One cautionary note bears mention: at *supersolidus* temperatures and at pressures below ~1.5 kbar, this model generates a complex set of phase relations among low-Ca pyroxenes. The complexities, which span a narrow range of temperature close to the experimentally determined solidi, include (1) the apparent reaction of Pig to Pen + Oen for compositions near 0.10 mole fraction $CaMgSi_2O_6$; (2) a singularity that arises from a calculated congruence in composition of Oen and Pig (expressed on isobaric sections as an azeotropic feature) above which Oen supplants Pig as the stable phase for compositions near 0.20 mole fraction; and (3) the apparent reaction of Pig to Oen + Dio for more calcic compositions. At ~1.5 kbar, the first two features listed above intersect in P-T projection,

eliminating the azeotrope from all higher-pressure equilibria; the third feature extends with steep positive dP/dT slope to ~5 kbar, where it terminates in a critical endpoint at its intersection with the Pig = Dio consolute curve. At pressures from ~2.5 to ~10 kbar and at temperatures near 1475–1500 °C, compositions in the range of ~0.05–0.10 mole fraction $CaMgSi_2O_6$ encounter the apparent reaction of Oen + Pen to produce Pig.

Because these complications appear principally at supersolidus temperatures and pressures, there is in fact no empirical evidence against their existence solely as features that are metastable with respect to a liquid phase. However, they are believed to have little petrologic significance, insofar as their existence and location are very strongly sensitive to small changes in the values of the thermodynamic parameters. Changes that do not materially affect the ability of the model to replicate the experimental data may greatly modify the calculated supersolidus equilibria. Nevertheless, although considerable effort was expended in an attempt to construct models in which these complications do not arise, no such model was simultaneously successful in fitting the entire range of experimental data. By acceptance of these complications in the present model, a choice has been made to meet the goal of closely fitting the existing experimental data, at the cost of limiting the confidence that can be placed in extrapolations beyond the experimental constraints, at least for supersolidus temperatures at low pressures.

Conclusion

The discussion above emphasizes the fact that the extraction of thermodynamic data from so thoroughly constrained a data set is a matter of successive compromises. For application to any limited range of conditions, a particular set of values for the parameters can be found that will provide a fit superior to the one derived here. Likewise, for applications in which closer correspondence to calorimetric or molar-volume data at 25 °C, 1 bar is required, a more suitable set of values can be found that will provide a more accurate replication of those data. The principal appeal of this new model, however, is the wide range of conditions over which it remains sufficiently accurate for geothermometric applications.

Acknowledgments

This work was funded by NSF Grants EAR-8603755 to W.D.C. and EAR-8416254 to D.H.L. The Geology Foundation of the University of Texas at Austin provided additional support. We thank David Andersen for helpful discussions and Paula Davidson for a most thoughtful review calling attention to some of the supersolidus phenomena described above.

References cited

Akaogi, M., and Akimoto, S. (1977) Pyroxene-garnet solid-solution equilibria in the systems $Mg_4Si_4O_{12}$-$Mg_3Al_2Si_3O_{12}$ and $Fe_4Si_4O_{12}$-$Fe_3Al_2Si_3O_{12}$ at high pressures and temperatures. Physics of the Earth and Planetary Interiors, 15, 90–106.

Atlas, Leon. (1952) The polymorphism of $MgSiO_3$ and solid-state equilibria in the system $MgSiO_3$-$CaMgSi_2O_6$. Journal of Geology, 60, 125–147.

Berman, R.G., and Brown, T.H. (1984) A thermodynamic model for multicomponent melts, with application to the system CaO-Al_2O_3-SiO_2. Geochimica et Cosmochimica Acta, 48, 661–678.

Brey, Gerhard, and Huth, J. (1984) The enstatite-diopside solvus to 60 kbar. Proceedings of the Third International Kimberlite Conference, 2, 257–264.

Carlson, W.D. (1985) Evidence against the stability of orthoenstatite above ~1005 °C at atmospheric pressure in CaO-MgO-SiO_2. Geophysical Research Letters, 12, 409–411.

——— (1986) Reversed pyroxene phase equilibria in CaO-MgO-SiO_2 at one atmosphere pressure. Contributions to Mineralogy and Petrology, 92, 218–224.

——— (1988) Subsolidus phase equilibria on the forsterite-saturated join $Mg_2Si_2O_6$-$CaMgSi_2O_6$ at atmospheric pressure. American Mineralogist, 73, 232–241.

Carlson, W.D., and Lindsley, D.H. (1986) A thermochemical model for proto-, ortho- and clinopyroxene in the system CaO-MgO-SiO_2. Geological Society of America Abstracts with Programs, 18, 558.

Chen, C.-H., and Presnall, D.C. (1975) The system Mg_2SiO_4-SiO_2 at pressures up to 25 kilobars. American Mineralogist, 60, 398–406.

Day, H.W., and Halbach, Heiner. (1979) The stability field of anthophyllite: The effect of experimental uncertainty on permissible phase diagram topologies. American Mineralogist, 64, 809–823.

Day, H.W., and Kumin, H.J. (1980) Thermodynamic analysis of the aluminum silicate triple point. American Journal of Science, 280, 265–287.

Gordon, Terry. (1977) Derivation of internally consistent thermochemical data from phase equilibrium experiments using linear programming. In H.J. Greenwood, Ed., Application of thermodynamics to petrology and ore deposits, p. 185–198. Mineralogical Association of Canada Short Course Handbook 2.

Grover, John. (1972) The stability of low-clinoenstatite in the system $Mg_2Si_2O_6$-$CaMgSi_2O_6$ (abs.). EOS, 53, 539.

Hawthorne, F.C., and Ito, Jun. (1977) Synthesis and crystal-structure refinement of transition-metal orthopyroxenes. I: Orthoenstatite and (Mg,Mn,Co) orthopyroxene. Canadian Mineralogist, 15, 321–338.

Holland, T.J.B., Navrotsky, Alexandra, and Newton, R.C. (1979) Thermodynamic parameters of $CaMgSi_2O_6$-$Mg_2Si_2O_6$ pyroxenes based on regular solution and cooperative disordering models. Contributions to Mineralogy and Petrology, 69, 337–344.

Kushiro, Ikuo, and Yoder, H.S., Jr. (1970) Stability field for iron-free pigeonite in the system $MgSiO_3$-$CaMgSi_2O_6$. Carnegie Institution of Washington Year Book, 68, 226–229.

Lindsley, D.H. and Dixon, S.A. (1976) Diopside-enstatite equilibria at 850 to 1400 °C, 5 to 35 kbars. American Journal of Science, 276, 1285–1301.

Lindsley, D.H., Grover, J.E., and Davidson, P.M. (1981) The thermodynamics the $Mg_2Si_2O_6$-$CaMgSi_2O_6$ join: A review and an improved model. In R.C. Newton, A. Navrotsky, and B.J. Wood, Eds., Thermodynamics of minerals and melts, p. 149–175. Springer-Verlag, New York.

Longhi, John, and Boudreau, A.E. (1980) The orthoenstatite liquidus field in the system forsterite-diopside-silica. American Mineralogist, 65, 563–573.

Mori, Takeshi, and Green, D.H. (1975) Pyroxenes in the system $Mg_2Si_2O_6$-$CaMgSi_2O_6$ at high pressure. Earth and Planetary Science Letters, 26, 277–286.

——— (1976) Subsolidus equilibria between pyroxenes in the CaO-MgO-SiO_2 system at high pressures and temperatures. American Mineralogist, 61, 616–625.

Nehru, C.E. and Wyllie, P.J. (1974) Electron microprobe measurements of pyroxenes coexisting with H_2O-undersaturated liquid in the join $CaMgSi_2O_6$-$Mg_2Si_2O_6$-H_2O at 30 kilobars, with applications to geothermometry. Contributions to Mineralogy and Petrology, 48, 221–228.

Newton, R.C., Charlu, P.A., Anderson, P.A.M., and Kleppa, O.J. (1979) Thermochemistry of synthetic clinopyroxenes in the join $CaMgSi_2O_6$-$Mg_2Si_2O_6$. Geochimica et Cosmochimica Acta, 43, 55–60.

Nickel, K.G., and Brey, Gerhard. (1984) Subsolidus orthopyroxene-clinopyroxene systematics in the system CaO-MgO-SiO_2 to 60 kbar: A

re-evaluation of the regular solution model. Contributions to Mineralogy and Petrology, 87, 35–42.

Perkins, Dexter, III, and Newton, R.C. (1980) The composition of coexisting pyroxenes and garnet in the system CaO-MgO-Al_2O_3-SiO_2 at 900–1100 °C and high pressures. Contributions to Mineralogy and Petrology, 75, 291–300.

Schweitzer, Elaine. (1982) The reaction pigeonite = $diopside_{ss}$ + $enstatite_{ss}$ at 15 kbars. American Mineralogist, 67, 54–58.

Smith, J.V. (1969) Crystal structure and stability of the $MgSiO_3$ polymorphs; physical properties and phase relations of Mg,Fe pyroxenes. Mineralogical Society of America Special Paper 2, 3–29.

Smyth, J.R. (1974) Experimental study on the polymorphism of enstatite. American Mineralogist, 59, 345–352.

Thompson, J.B., Jr. (1967) Thermodynamic properties of simple solutions. In P.H. Abelson, Ed., Researches in geochemistry, 2, 340–361. Wiley, New York.

Warner, R.D., and Luth, W.L. (1974) The diopside-orthoenstatite two-phase region in the system $CaMgSi_2O_6$-$Mg_2Si_2O_6$. American Mineralogist, 59, 98–109.

Manuscript received July 27, 1987
Manuscript accepted November 13, 1987